ABC Importers

Lotteke J.Y.M. Swier, Dirk-Jan Slotboom and Bert Poolman

Abstract Most ABC importers employ a soluble substrate-binding protein (SBP) to capture the ligand and donate the molecule to the translocator. The SBP can be a soluble periplasmic protein or tethered to the membrane via a lipid moiety or protein anchor or fused to the translocator. In the hybrid ABC transporters, multiple substrate-binding domains (SBDs) can be fused in tandem and provide several extracytoplasmic substrate-binding sites. The substrate is transferred from the SBP to the membrane domain, which translocates the substrate via alternating access of a membrane-embedded substrate-binding pocket. A subset of ABC transporters, known as the energy-coupling factor (ECF) transporters, employs a membrane-embedded S-component to capture the substrate. The S-component guided by the ECF module transports the substrate over the membrane via a so-called toppling mechanism. An overview of the mechanisms of transport by the different types of ABC importers is presented, together with structural information about the proteins.

Introduction

ATP-binding cassette (ABC) proteins serve many functions, including the transport of nutrients into the cell, transport of compounds across organellar membranes, the secretion of proteins, antigen (peptide) presentation, cell volume regulation, regulation of protein synthesis, detoxification, and antibiotic resistance. The vast majority of ABC proteins are part of complexes that mediate transport of molecules across cellular or organellar membranes. A smaller group of ABC proteins is associated with soluble (supra) molecular complexes and involved in DNA repair, recombination, chromosome condensation and segregation, and translation elongation. Regardless

L.J.Y.M. Swier · D.-J. Slotboom · B. Poolman (✉)
Department of Biochemistry, University of Groningen, Groningen Biomolecular Sciences and Biotechnology Institute and Zernike Institute for Advanced Materials, Nijenborgh 4, 9747, AG Groningen, The Netherlands
e-mail: b.poolman@rug.nl

A.M. George (ed.), *ABC Transporters—40 Years on*,
DOI 10.1007/978-3-319-23476-2_1

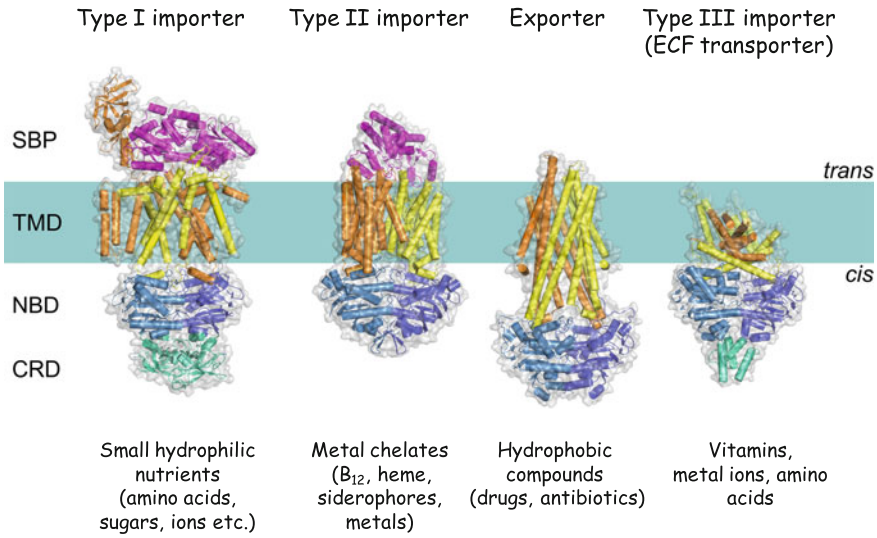

Fig. 1 ABC superfamily of transporters: Type I, II, and III importers and exporters. The TMDs are colored *orange* and *yellow*, the NBDs *light* and *dark blue*, and additional domains which often have a regulatory function, are colored *green*. The SBPs are in *purple*. From Ter Beek et al. (2014)

of whether the ABC proteins are found in membrane transport or soluble (supra) molecular complexes, they provide a power stroke in which chemical energy is converted into work (e.g., for a translocation or dislocation event).

ABC transporters are subdivided into importers and exporters. Both importers and exporters consist of two transmembrane domains (TMDs) and two cytoplasmic nucleotide-binding domains (NBDs), which power the transport through hydrolysis of ATP. The TMDs and NBDs together form the translocator. In this chapter we focus on ABC importers, which on structural and mechanistic grounds are subdivided into Type I, II, and III importers (Fig. 1) (Ter Beek et al. 2014). The mechanism of transport of Type I and II ABC importers involves the binding and release of substrate from a dedicated extracytoplasmic substrate-binding protein (SBP) and alternating access of the substrate-binding pocket in the translocator domain. Type III importers, also named energy-coupling factor (ECF) transporters, capture ligands via so-called S-components, which are small integral membrane proteins that associate with a transmembrane coupling protein and two NBDs to form a full transporter; the different types of modularity are presented in Box I. The mechanism of transport of Type III importers may involve substrate translocation by toppling of the S-component rather than alternating access of the translocator domain. The current status of the mechanisms of transport by Type I, II, and III importers is presented in separate sections below, but we first introduce the substrate-binding proteins associated with Type I and II importers and a recently proposed classification of these important accessory proteins.

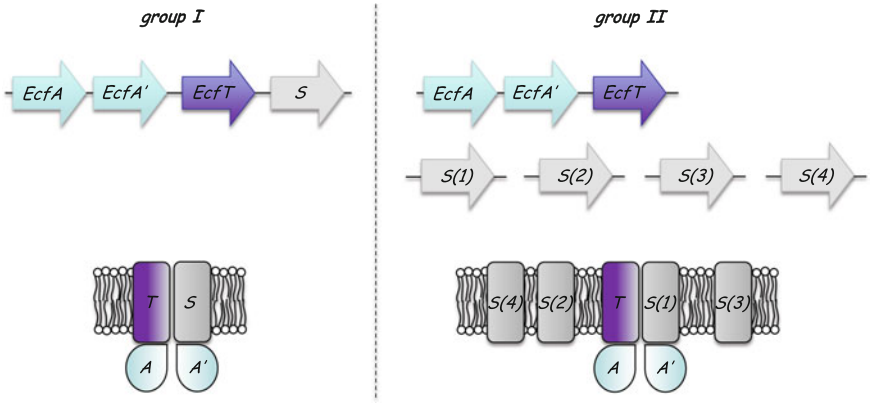

Fig. 2 Schematic representation of group I and group II ECF transporters, showing both the chromosomal location of the genes as well as the architecture of the transporters. After Slotboom (2014)

Box I: Classification within Type III ABC importers
Like the Type I and Type II ABC importers, the Type III importers consist of two identical or highly similar cytoplasmic NBDs (EcfA and EcfA') and two TMDs. One of the TMDs is called the S-component and functions as the substrate-binding protein. The other three subunits form the eponymous ECF module and fuel transport by ATP binding and hydrolysis. Based on the chromosomal location of the genes encoding all four subunits, the ECF transporters are subdivided into group I and group II. In group I transporters, the genes encoding all four subunits are present in one operon and under the control of a single promotor; the gene products form a dedicated transporter. In group II transporters, the genes for the ECF module are clustered together, while genes encoding S-components for different substrates are scattered around the genome. These S-components are all able to interact with the same ECF module. This modularity is analogous to the promiscuity of a subset of Type I importers that can interact with different SBPs or have multiple different SBDs fused to their TMD (Fig. 2).

Structural Features of Substrate-Binding Proteins

Substrate-binding proteins were first discovered in the periplasm of *Escherichia coli* (Berger and Heppel 1974), a Gram-negative bacterium, and are still often referred to as periplasmic binding proteins. A recent proteomics study showed that up to 80 % of the proteins of the periplasm of *E. coli* can be SBPs depending on the

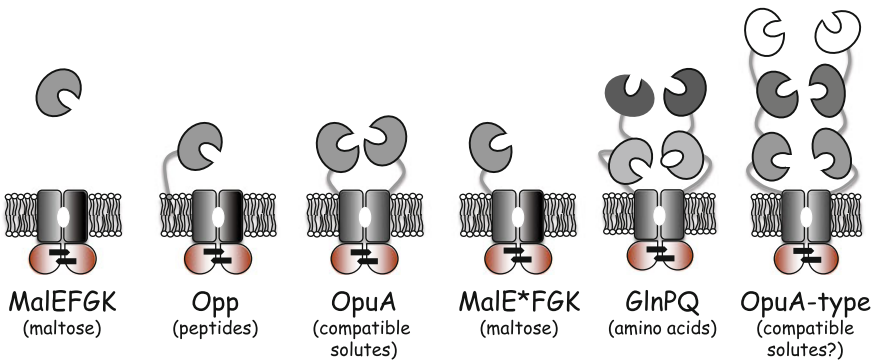

Fig. 3 Types of Type I ABC importers. The TMDs are colored *gray* and the associated SBPs or covalently linked SBDs are shown in different *shades of gray* (from *white* to *dark gray*); the NBDs are colored *orange* and two molecules of ATP are indicated by bars. After van der Heide and Poolman (2002)

growth conditions, with the number of most SBPs increasing with decreasing growth rate (Heinemann et al., unpublished). Thus, cells express more SBPs when nutrient conditions become harsh. In a few cases a limited number of related SBPs can associate with the same translocator (Davidson et al. 2008), enabling the system to import multiple distinct substrates. The first SBP crystal structure, the L-arabinose-binding protein (ABP), was solved in 1974 (Quiocho et al. 1974).

The soluble SBPs of Type I importers are present in large excess over the translocator complexes in the membrane, allowing efficient capture of substrates and initiation of the translocation reaction (Heinemann et al., unpublished). In contrast, the SBPs of Type II importers appear to be stoichiometric with the translocators. In Gram-positive bacteria and archaea, i.e., microorganisms lacking an outer membrane and periplasm, SBPs are exposed on the cell surface and attached to the cytoplasmic membrane via a lipid anchor or a transmembrane peptide (observed in archaea only), or they can be fused to the TMDs. The latter has been observed in hetero- and homodimeric TMDs, and thus results in one or two SBDs per functional complex (van der Heide and Poolman 2002; Schuurman-Wolters and Poolman, unpublished). In some cases, two or even three SBDs fused in tandem are linked to the TMDs and these systems have a total of four or six extracytoplasmic substrate-binding sites (Fig. 3). Systems with SBDs fused to the TMDs can also be found in Gram-negative bacteria but less frequently compared to Gram-positive bacteria (van der Heide and Poolman 2002). The linking of SBDs to the membrane or the fusion of multiple SBDs to the TMD increases the effective concentration of the substrate-binding sites near the translocator and increases the efficiency of transport (Schuurman-Wolters and Poolman, unpublished). The relatively short (10–20 amino acid) flexible linkers allow the SBDs to probe a small volume around the translocator, leading to an effective concentration of the SBDs in the millimolar range. The affinity of the fused SBDs for the translocator is not known, but the dissociation constants might be millimolar or higher. In case of

soluble or lipid-anchored SBPs, the affinity for the translocator is ~0.1 mM when the proteins are in the closed-liganded state (Prossnitz et al. 1989; Dean et al. 1992; Doeven et al. 2004). These low affinities may necessitate a high concentration of SBPs in the periplasm [the maltose-binding protein reaches a concentration of ~1 mM; Manson et al. (1985)] or surface-tethering of the proteins. Given that the periplasm is highly crowded and diffusion is slow (diffusion coefficients for proteins of the size of SBPs in the periplasm are even lower than in the cytoplasm; van den Berg et al., unpublished) and synthesizing a large excess of SBPs is costly, it is perhaps surprising that the covalent linking of SBDs is not more widespread or even universal for ABC importers. The mechanism of substrate binding of periplasmic, membrane-anchored, and TMD-fused SBDs is similar and so is the mode of action of the corresponding ABC transporters (vide infra).

SBPs consist of two lobes connected by a linker or hinge (domain). The two lobes close and engulf the ligand upon substrate binding (mode of substrate capture akin that of a Venus's Flytrap) (Quiocho and Ledvina 1996). Structures are available of SBPs in the open-unliganded (O), closed-unliganded (C), open-liganded (OL), and closed-liganded (CL) forms; the latter conformation is thought to productively interact with the translocator complex. Mutational and structural analyses indicate that each lobe of the SBP binds to one of the TMDs (Hollenstein et al. 2007a; Davidson et al. 2008), and conformational changes in the NBDs upon binding of ATP are transmitted via the TMDs to the SBP. Thus, ATP is involved in the opening of the SBPs and substrate transfer to the translocator.

SBPs associated with ABC transporters are related to similar domains present in a wide variety of translocation and signal transduction systems in both prokaryotic and eukaryotic organisms, including tripartite ATP-independent periplasmic (TRAP) transporters, two-component regulatory systems, guanylate cyclase–atrial natriuretic peptide receptors, G-protein coupled receptors (GPCRs), and ligand-gated ion channels (Berntsson et al. 2010). In addition, SBDs are part of prokaryotic DNA-binding proteins involved in gene regulation. SBPs are very diverse in sequence, and phylogenetic analyses based on multiple sequence alignments do not yield stable alignments (the sequence identity of the proteins is often < 20 %). However, the structures of SBPs are remarkably similar, which has been used to cluster the SBPs based on structural similarity instead of sequence similarity (Berntsson et al. 2010).

Pairwise structural alignments of more than 100 SBPs have been used to produce a structural distance tree. The SBPs were found to group into six defined clusters (A–F), three of which (clusters A, D, and F) were further subdivided. The analyses have shown that the proteins within the six clusters can be discriminated on the basis of the linker (hinge) region that connects the two protein lobes (Fig. 4): the generic secondary structure is $(\beta)_{4/5}(\alpha)_n$-hinge-$(\beta)_{4/5}(\alpha)_n$ (Fukami-Kobayashi et al. 1999). There is little or no correlation between the structural clustering and functional classification, that is, SBPs with very different substrate specificities are present in each cluster. Furthermore, in the individual clusters, the proteins are not necessarily homologous, as judged from the absence of significant sequence

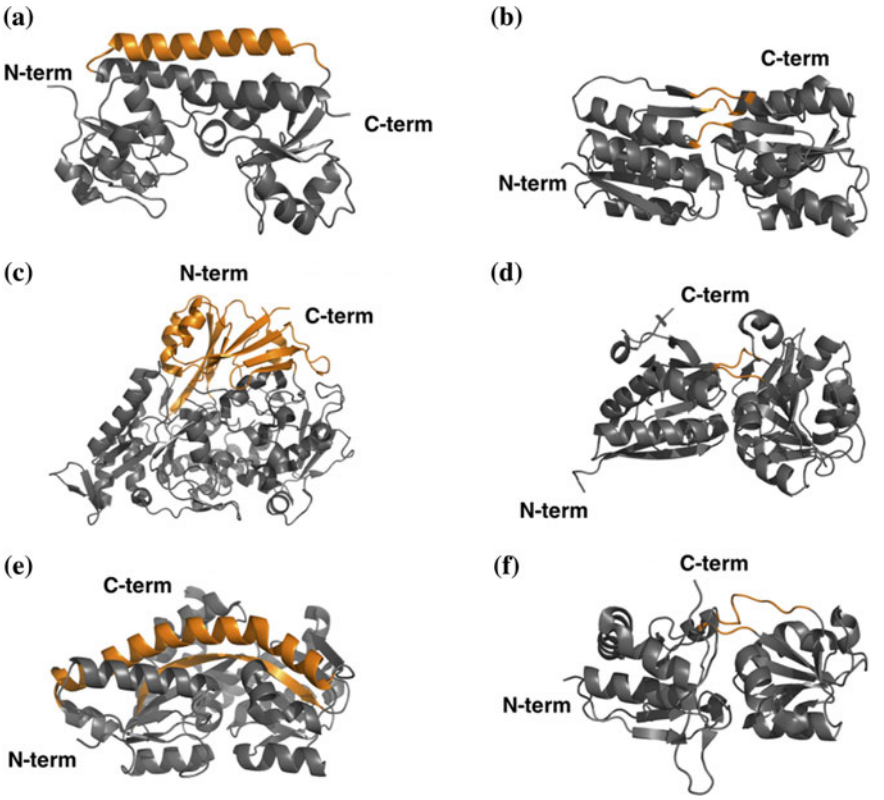

Fig. 4 The different clusters of SBPs are shown with their distinct structural features colored in *orange*. **a** Cluster A contains SBPs having a single connection between the two domains in the form of a rigid helix. **b** Cluster B contains SBPs with three interconnecting segments between the two domains. **c** Cluster C contains SBPs that have an extra domain and are significantly larger in size when compared with the others. **d** Cluster D contains SBPs with two relatively short hinges. **e** Cluster E contains SBPs associated with TRAP transporters which all contain a large helix functioning as the hinge region. **f** Cluster F contains SBPs with two hinges similarly like those of cluster D, however, these hinges have almost double the length creating more flexibility inside the SBP. Please note that Clusters A, D, and F can further be subdivided based on the substrate of the SBP (see text). The proteins used to illustrate the features in Cluster A–F are BtuF (PDB code: 1N2Z), RBP (PDB code: 1DRJ), OppA (PDB code: 3DRF), ModA (PDB code: 1ONR), UehA (PDB code: 3FXB), and HisJ (PDB code: 1HSL), respectively. Figure was taken from Berntsson et al. (2010)

similarity. Clusters B and F contain the most diverse SBPs, associated with various types of transport and signal transduction systems; SBPs in cluster A are unique to type II ABC importers; clusters C and D contain SBPs of Type I ABC importers; and SBPs in cluster E are found in TRAP transporters. Specific information on the six clusters is presented in Box II.

Box II: Structural features distinguishing substrate-binding proteins

Cluster A: The cluster A SBPs associate with Type II ABC importers. The distinguishing characteristic of these SBPs is an α-helix that serves as a hinge between the two domains. The rigidity of this helix is reflected in the small movement of both domains upon substrate binding. All of the SBPs in cluster A play a role in metal binding, either directly or as metal chelates.

Cluster B: Cluster B consists of SBPs that bind carbohydrates, branched chain amino acids, natriuretic peptides, and autoinducer-2 (AI-2). The SBPs in cluster B interact with type I ABC importers, two-component histidine-sensory complexes, and guanylate cyclase-atrial natriuretic peptide receptors. The hinge of the SBPs in cluster B is built of three distinct regions connecting the lobes. Homologous to the proteins in cluster B are the *lac*-repressor type transcription factors.

Cluster C: The cluster C SBPs interact with Type I ABC importers and bind diverse ligands including di- and oligopeptides, arginine, nickel ions, and cellobiose. They all have an extra domain, which in oligopeptide transporters extends the binding cavity to accommodate very large ligands (peptides of 20 residues or more).

Cluster D: The discernible feature of these proteins is that their hinge region consists of two short stretches, 4–5 amino acids long. This large group of SBPs binds a large variety of substrates: carbohydrates, putrescine, thiamine, tetrahedral oxyanion as well as ferric or ferrous iron.

Cluster E: These SBPs are part of the TRAP transporter (tripartite ATP-independent periplasmic transporter) family. TRAP transporters use an electrochemical ion gradient to fuel the uphill translocation of substrates. The remarkable feature of TRAP SBPs is a large single ß-strand that is part of the two five-stranded ß-sheets of both lobes. All TRAP-dependent SBPs structurally characterized have a conserved strand order, typical of class II SBPs ($\beta_2\beta_1\beta_3\beta_n\beta_4$), and an additional ß-strand connecting both domains. A second distinguishing feature is a long helix that spans both domains, although in some structures it is interrupted by a kink. The known substrates are ectoine, pyroglutamic acid, lactate, 2-keto acids, and sialic acid.

Cluster F: The distinguishing feature of the cluster F proteins is a hinge consisting of two segments connecting the two lobes. The linker stretches of cluster F proteins are significantly longer (8–10 amino acids) than the hinges of 4–5 amino acids observed in SBPs of cluster D. Possibly the longer linker provides more flexibility between the open and closed conformation. Cluster F SBPs bind a large variety of substrates ranging from trigonal planar anions (nitrate, bicarbonate) to amino acids and compatible solutes such as glycine betaine.

Mechanism of Ligand Binding

SBPs have been captured in crystals in different conformations: open (O) and closed (C), either with or without ligand (L). In solution, the equilibrium state of the SBPs is toward the open (O) conformation in the absence of ligand and toward the closed conformation in the presence of ligand (CL). The crystal structures provide crucial snapshots of different conformational states of the SBPs, but they do not reveal the dynamics of ligand binding. Different models for ligand binding are possible. In the *induced fit* mechanism, the initial interaction between protein and ligand (OL) is relatively weak but triggers the closing of the protein and formation of CL (Fig. 5). In the *conformational selection* mechanism, the protein samples closed states (partially closed (PC) or fully closed (C) in Fig. 5) without the involvement of a ligand. Ligand binding stabilizes the PC or C-form and thereby drives the equilibrium to the closed form CL. A combination of both mechanisms is also possible, but nowadays it is thought that conformational selection is the dominant mechanism of ligand binding by enzymes and receptors (Vogt and Di Cera 2013; Clore 2014).

The two mechanisms make specific predictions about the kinetics of ligand binding, i.e., the closing rate increases with ligand concentration in *induced fit* but not in *conformational selection* (Fig. 5). Moreover, in the *conformational selection* mechanism, the life-time of the closed state increases with ligand concentration. To discriminate between *induced fit* and *conformational selection* is generally not possible in ensemble measurements because differences in conformations are averaged out. Single-molecule observations with high time resolution allow the two mechanisms or hybrid forms to be discriminated. Recent single-molecule Förster resonance energy transfer (smFRET) studies of the maltose-binding protein (MalE)

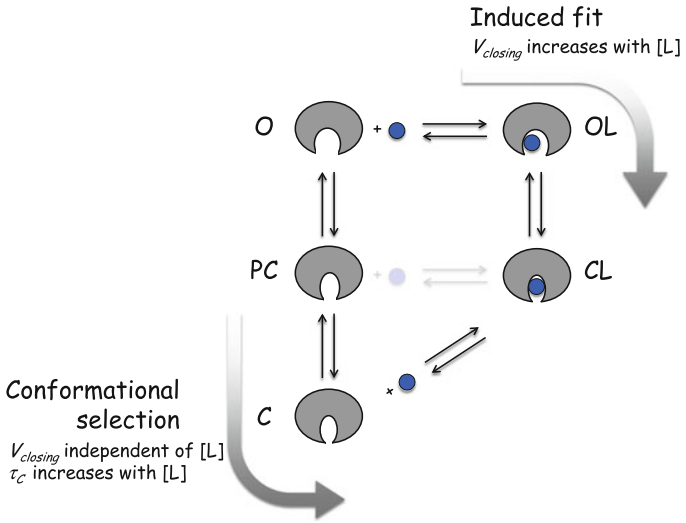

Fig. 5 Ligand-binding mechanisms. Conformational transitions in SBDs according to the induced fit or the conformational selection binding mechanism, as explained in the main text. V_{closing}, rate of closing of the binding site; τ_c, life-time of the closed state; and [L], ligand concentration

(Kim et al. 2013; Seo et al. 2014) and the two SBDs of the amino acid ABC importer GlnPQ (Gouridis et al. 2015) have shown that these proteins bind their ligands by a previously undocumented type of *induced fit* mechanism: the SBDs intrinsically transit from O to C in addition to being triggered to close by the ligand. Remarkably, as shown for both SBDs from GlnPQ, the life-time of C is the same as that of CL when high-affinity ligands (with sub-micromolar dissociation constants) are bound. In contrast, the life-time of CL is dramatically shortened when low-affinity ligands are bound. This observation indicates that the ligands do not "stabilize" the closed conformation, which is often thought on the basis of the multiple interactions between protein and ligand in crystal structures.

Box III. The GlnPQ transporter

The GlnPQ transporter from *Lactococcus lactis* and other Gram-positive bacteria has homodimeric TMDs with two SBDs fused in tandem to each of them (Fig. 3, 6th cartoon). The N-terminal SBD (SBD1) is preceded by a signal sequence that is cleaved off following translocation of the SBDs across the membrane (Schuurman-Wolters and Poolman 2005).

Thus, in GlnPQ four SBDs compete for interaction with the translocator to deliver the bound ligand. The close proximity of multiple SBDs, each of which can adopt different conformations (O, C, OL, or CL) and close intrinsically, affects transport (Gouridis et al. 2015). GlnPQ imports asparagine solely via SBD1 (K_D = 0.2 μM), and glutamine via both SBD1 (K_D ∼ 100 μM) and SBD2 (K_D = 1 μM), but with affinities that differ by two orders of magnitude (Fulyani et al. 2013). The transport of asparagine has been determined in the absence of glutamine (SBD2 ∼ 98 % in O, ∼2 % in C), in the presence of relatively low concentrations of glutamine that do not significantly compete with Asn for binding to SBD1 (SBD2 > 95 % in CL), and in the absence or presence of glutamine and a mutation (D417F) that prevents SBD2 from binding ligand and, more importantly, prevents closing (SBD2 ∼ 100 in O) (Gouridis et al. 2015). The remarkable observation was made that the D417F mutation increases the rate of asparagine import by a factor of 3, showing that 2 % of C already has a strong inhibitory effect on transport via SBD1. In fact, the inhibition of asparagine transport via SBD1 by 2 % of SBD2 in the C state is comparable to the inhibition by 95 % in the CL.

These experiments indicate that the TMDs interact with the closed state of the SBD, but the interaction is shorter-lasting for CL (leading to a productive translocation cycle) than for C (leading to a long-lived blocked intermediate state). This work illustrates the importance of understanding the mechanism of ligand binding to substrate-binding proteins in order to begin to understand the full translocation cycle. Although not so easily probed in ABC importers with periplasmic or lipid-anchored SBPs, similar kinetics of ligand binding and competition between proteins in different conformation states could play a role in these systems.

Structural Features of ABC Importers

Type I Importers

Crystal structures of Type I importers for four different substrates are available: the molybdate/tungstate transporter $ModB_2C_2$ from *Archaeoglobus fulgides* (Hollenstein et al. 2007b) and *Methanosarcina acetivorans* (Gerber et al. 2008), the maltose transporter $MalFGK_2$ from *E. coli* (Oldham et al. 2007, 2013; Khare et al. 2009; Oldham and Chen 2011a, b; Chen et al. 2013), the methionine transporter $MetN_2I_2$ from *E. coli* (Kadaba et al. 2008; Johnson et al. 2012), and the transporter for basic amino acids $Art(QN)_2$ from *Thermoanaerobacter tengcongensis* (Yu et al. 2015). $MalFGK_2$ is by far the most studied transporter. The different crystal structures are listed in Table 1.

The crystal structure of $MalFGK_2$ in the inward-facing apo-state is likely representing the resting state of the transport cycle (Khare et al. 2009). The two TMDs of $MalFGK_2$, MalF and MalG, are not identical. They consist of eight and six transmembrane helices, respectively, from which TM3-8 of MalF are related to TM1-6 of MalG. These helices form the core region of the TMDs with pseudo-twofold symmetry. In the inward-facing state, the interface between MalF and MalG creates a translocation cavity, which is accessible from the cytoplasm. On the periplasmic end, this cavity is closed by a periplasmic, hydrophobic gate that is composed of four loops, each at the kink of a transmembrane helix (TM5 and TM7 from MalF, TM3 and TM5 from MalG). Both MalF and MalG have a coupling helix, which is located in loop L6 between TM6 and TM7 of MalF and in loop L4 between TM4 and TM5 of MalG. Both coupling helices dock into a groove on the surface of each of the two NBDs (MalK subunits). These grooves are lined by two helices from the helical subdomain of MalK, the helix following the Walker A motif and residues from the Q-loop. The interactions between the coupling helices and the MalK subunits transduce conformational changes upon ATP binding and hydrolysis to MalF and MalG and allow alternate access of the binding pocket in the TMDs.

Within the MalF–MalG dimer, an occluded maltose-binding pocket is formed about halfway the membrane. In the structures showing maltose-bound $MalFGK_2$ in a pre-translocation state (Oldham and Chen 2011a), this pocket is closed at the periplasmic side by a hydrophobic gate. On the cytoplasmic side, the pocket is closed by a network of van der Waals interactions. The binding pocket is lined by residues from MalF only, and the binding mode resembles that of MBP in terms of aromatic stacking of binding site residues with the sugar rings, as well as a hydrogen-bond network involved in sugar recognition.

A crystal structure of nucleotide-free $MalFGK_2$–MBP in the pre-translocation state with maltoheptaose bound has shed light on the selectivity of sugar transport (Oldham et al. 2013). $MalFGK_2$ imports linear malto-oligosaccharides of a length from two to seven glycosyl units, linked through α-1,4 glycosidic bonds, with an unmodified reducing end. In the crystal structure, four glycosyl units from the

Table 1 The different crystal structures available of ABC importers

Name (organism)	Remarks	Substrate bound	Resolution (Å)	PDB code	Reference
Type I importers					
Molybdate transporter $ModB_2C_2$ in complex with ModA (*Archaeoglobus fulgidus*)	Inward-facing conformation, with SBP	Mg^{2+}, PO_4^{3-}, WoO_4^{2-}	3.10	2ONK	Hollenstein et al. (2007a, b)
Molybdate ABC transporter ModBC in a *trans*-inhibited state (*Methanosarcina acetivorans*)	Inward-facing conformation, without SBP bound	Mg^{2+}, WoO_4^{2-}	3.00	3D31	Gerber et al. (2008)
Maltose transporter $MalFGK_2$ in complex with MBP (*Escherichia coli*)	Outward-facing conformation stabilized by a mutation in the NBDs (MalK E159Q)	Maltose, ATP	2.80	2R6G	Oldham et al. (2007)
Maltose transporter $MalFGK_2$ (*E. coli*)	TM helix 1 deleted, in inward-facing conformation, in resting state, without MBP	–	4.50	3FH6	Khare et al. (2009)
Maltose transporter $MalFGK_2$ in complex with MBP (*E. coli*)	Pre-translocation intermediate state, with MBP	AMP–PNP, Mg^{2+}, maltose	2.90	3PUZ	Oldham and Chen (2011a)
After crystal soaking	Pre-translocation, outward-facing conformation, with MBP	AMP–PNP, Mg^{2+}, maltose	3.10	3PUY	
With mutations in MBP	Pre-translocation intermediate state with mutations in MBP (G69C/S337C) that stabilize the substrate-bound closed conformation by a crosslink	Maltose	3.10	3PV0	
Maltose transporter $MalFGK_2$ in complex with MBP (*E. coli*)	Outward-facing conformation with MBP	AMP–PNP, Mg^{2+}, maltose	2.20	3RLF	Oldham and Chen (2011b)
With orthovanadate	Outward-facing conformation, ADP in conjunction with vanadate, with MBP	ADP · VO_4^{3-}, Mg^{2+}, maltose	2.40	3PUV	
With tetrafluoroaluminate	Outward-facing conformation, ADP in conjunction with tetrafluoroaluminate, with MBP	ADP · AlF_4^-, Mg^{2+}, maltose	2.30	3PUW	
With beryllium trifluoride	Outward-facing conformation, ADP in conjunction with beryllium trifluoride, with MBP	ADP · BeF_3^-, Mg^{2+}, maltose	2.30	3PUX	
			3.91	4JBW	

(continued)

Table 1 (continued)

Name (organism)	Remarks	Substrate bound	Resolution (Å)	PDB code	Reference
Maltose transporter $MalFGK_2$ in complex with MBP (*E. coli*)	Complex with regulatory protein $EIIA^{glc}$, inward-facing conformation				Chen et al. (2013)
Maltose transporter $MalFGK_2$ in complex with MBP (*E. coli*)	Pre-translocation conformation; maltoheptaose bound	Maltoheptaose	2.90	4KHZ	Oldham et al. (2013)
	Pre-translocation, outward-facing conformation	ANP, α-D-glycose	2.38	4KI0	
Methionine transporter $MetN_2I_2$ (*E. coli*) (dodecylmaltoside-purified)	Inward-facing conformation	–	3.70	3DHW	Kadaba et al. (2008)
At higher resolution (Cymal5-purified)	Inward-facing conformation	ADP	2.90	3TUI	Johnson et al. (2012)
(decylmaltoside-purified)	Inward-facing conformation, C2 domains repositioned	–	4.00	3TUJ	
Se-Methionine soaked (Cymal5-purified)	Inward-facing conformation	ADP	3.40	3TUZ	
Amino acid transporter $Art(QN)_2$ (*Thermoanaerobacter tengcongensis*)	Inward-facing conformation	–	2.80	4YMS	Yu et al. (2015)
With arginine	Inward-facing conformation	Arginine	2.59	4YMT	
With ATP and arginine	Inward-facing conformation	ATP, arginine	2.50	4YMU	
With ATP	Inward-facing conformation	ATP	3.00	4YMV	
With histidine	Inward-facing conformation	Histidine	2.80	4YMW	
Type II importers					
Vitamin B_{12} transporter BtuCD (*E. coli*)	Outward-facing conformation, no SBP bound	$V_4O_{12}^{4-}$	3.20	1L7V	Locher et al. (2002)
With nucleotide	Outward-facing conformation	AMP–PNP	2.79	4R9U	Korkhov et al. (2014)
Vitamin B_{12} transporter BtuCD in complex with BtuF (*E. coli*)	Intermediate occluded state. The translocation pore is closed from both sides. BtuF is in an open state	–	2.60	2QI9	Hvorup et al. (2007)

(continued)

Table 1 (continued)

Name (organism)	Remarks	Substrate bound	Resolution (Å)	PDB code	Reference
Vitamin B_{12} transporter BtuCD in complex with BtuF with mutation in NBD (*E. coli*)	E159Q mutation abolished ATP hydrolysis activity, BtuC in asymmetric conformation	–	3.49	4DBL	Korkhov et al. (2012a)
Vitamin B_{12} transporter BtuCD in complex with BtuF (*E. coli*)	Intermediate state	AMP–PNP	3.47	4FI3	Korkhov et al. (2012b)
Putative metal-chelate-type ABC transporter HI1470/1471 (*Haemophilus influenzae*), later renamed $MolB_2C_2$ (when shown to bind WoO_4^{2-}/MoO_4^{2-})	Inward-facing conformation, without SBP	–	2.40	2NQ2	Pinkett et al. (2007)
Heme transporter HmuUV (*Yersinia pestis*)	Outward-facing	–	3.00	4G1U	Woo et al. (2012)
ECF-type importers					
RibU S-component for riboflavin (*Staphylococcus aureus*)	Substrate bound	Riboflavin	3.60	3P5N	Zhang et al. (2010)
ThiT S-component for thiamin (*Lactococcus lactis*)	Substrate bound	Thiamin	2.00	3RLB	Erkens et al. (2011)
BioY S-component for biotin (*Lactococcus lactis*)	Substrate bound	Biotin	2.10	4DVE	Berntsson et al. (2012)
NikM S-component for Ni^{2+} (*Thermoanaerobacter tengcongensis*)	Substrate bound	Ni^{2+}/Co^{2+}	2.50, 1.83, 3.21	4M5C, 4M5B, 4M58	Yu et al. (2014)
CbiO homodimer of CbiMNQO (*Thermoanaerobacter tengcongensis*)	Nucleotide free	–	2.30	4MKI	Chai et al. (2013)

(continued)

Table 1 (continued)

Name (organism)	Remarks	Substrate bound	Resolution (Å)	PDB code	Reference
EcfAA' heterodimer (*Thermotoga maritima*)	Nucleotide bound	ADP	2.70	4HLU	Karpowich and Wang (2013)
Folate ECF transporter (*Lactobacillus brevis*)	Substrate free	–	3.00	4HUQ	Xu et al. (2013)
Putative Pdx ECF transporter (*Lactobacillus brevis*)	Substrate free	–	3.53	4HZU	Wang et al. (2013)
Pantothenate ECF transporter (*Lactobacillus brevis*)	Substrate free	–	3.25	4RFS	Zhang et al. (2014)

reducing end of maltoheptaose are bound in the groove between the N-terminal and C-terminal lobe of MBP. A conserved glutamine in the periplasmic L5 loop of MalG is also inserted into this groove and forms hydrogen bonds with the first glycosyl unit at the reducing end. There is no clear electron density found for the glycosyl units at the non-reducing end of maltoheptaose. In a different AMP–PNP bound, pre-translocation state structure with an outward-facing conformation, three glucosyl units from the non-reducing end of maltoheptaose are bound in the MalF-binding site (Oldham et al. 2013). Aromatic stacking interactions and five direct protein–sugar hydrogen bonds within this binding site indicate specificity for α-1,4 linkage of the glycosyl units. The other glucosyl units of maltoheptaose are not visible, probably because they do not have specific interactions with the transporter. Overall, it seems that the size-exclusion limit of transport by $MalFGK_2$ is determined by the size of the cavity in the occluded state, which is about 2400 Å, just large enough to fit a maltoheptaose molecule.

Five crystal structures of the transporter for basic amino acids $Art(NQ)_2$ from *T. tengcongensis* in the apo-, arginine-, histidine-, ATP-, and ATP plus arginine-bound state all show an inward-facing conformation, with the nucleotide-binding domains (ArtNs) in a semi-open state (Yu et al. 2015). The transmembrane domains (ArtQs) contain five transmembrane segments, which correspond to TM4-8 of MalF and TM2-6 of MalG, and form a homodimer with twofold symmetry. Together, the ArtQs form a highly negatively charged tunnel reaching from the periplasmic side to the cytoplasmic side of the membrane, which allows positively charged amino acids to pass through. Halfway across the predicted membrane, each ArtQ subunit has a highly negatively charged substrate-binding pocket, lined by highly conserved residues that are involved in specific binding of both arginine and histidine. Remarkably, two amino acids are present in the ArtQ dimer, which raises questions on the transport mechanism as one amino acid at a time is transferred from the substrate-binding protein ArtI to $Art(NQ)_2$. A crystal structure of ArtI in the arginine bound state shows only one binding site. We therefore consider it more likely that the two amino acids have accessed the binding pocket when the protein was trapped in the inward-facing conformation, and that the structures do not reflect a true translocation intermediate.

Capturing $MalFGK_2$ in an ATP-bound state was achieved by mutating the catalytic glutamate in the ATP hydrolysis site to a glutamine (E159Q) (Oldham et al. 2007). In the outward-facing conformation, the translocation cavity is now open to the bound MBP, which is in a substrate-free state (Oldham et al. 2007; Oldham and Chen 2011a, b). On the cytoplasmic side, the translocation cavity is closed by a tightly packed helix bundle of TM6 and TM7 from MalF and TM4 and TM5 from MalG. In the pre-translocation, occluded state, only four residues from these TMs are forming the gate. In the closed, nucleotide-bound MalK dimer, two ATP or AMP-PNP molecules are sandwiched at the dimeric interface, where they interact with residues from the Walker A and Walker B motifs of one MalK subunit and residues from the LSGGQ signature sequence of the other subunit. Compared to the pre-translocation, occluded state, the helical domains of the NBDs have rotated another 15°, thereby breaking the intersubunit hydrogen-bond network of

the MalK dimer. Overall, when comparing the inward-facing and outward-facing conformations, the structures of the core helices TM4-7 in MalF and TM2-5 in MalG are maintained as rigid bodies during the transport cycle. The other helices, TM2, TM3, and TM8 of MalF and TM1 and TM6 of MalG, move together with the core helices of the other TMD subunit. The helical domains of the NBDs, as well as the coupling helices, rotate over an angle of about 30° upon closure of the MalK dimer, which allows the conformational change in the MalFG dimer.

$MalFGK_2$ has been crystallized in complex with the MBP, maltose, and ADP together with phosphate analogs VO_4^-, AlF_4^-, or BeF_3^-, which has provided insight into the mechanism of ATP hydrolysis within the MalK dimer (Oldham and Chen 2011b). The overall structures show the same outward-facing conformation as described above, suggesting that ATP hydrolysis does not force the transporter in a different conformation. Even the conserved residues within the ATP hydrolysis site are superimposable on all four structures. The hydrolysis of ATP proceeds by the attack of the γ-phosphate of ATP by a water molecule, which is thought to transit a pentacovalent intermediate state. The VO_4^- and AlF_4^- bound structures show a trigonal bipyramidal and octahedral geometry, respectively, which represent the transition state of the hydrolysis. Three of the four oxygen atoms of VO_4^- or the fluorides of AlF_4^- lie in the equatorial plane, while the fourth oxygen of VO_4^- or the attacking water molecule in case of the AlF_4^- bound structure and the oxygen connecting the β-phosphate group are found at the axial positions. This transition state supports the catalysis-by-a-general-base model, where the attacking water molecule is activated by the conserved glutamate (E159) by polarizing the water molecule. The conserved histidine (H192) in the H-loop positions the γ-phosphate group, the attacking water molecule, and the conserved glutamate, while the conserved glutamine (Q82) in the Q-loop is involved in coordination of the Mg^{2+} ion.

In the final step before returning to the resting state, the SBP is released from the transporter and the inorganic phosphate and ADP are released from the NBDs. Intermediate states of this step are observed in the crystal structure of the molybdate/tungstate transporter $ModB_2C_2$ from *A. fulgides,* which is in the inward-facing conformation in complex with its substrate-binding protein ModA (Hollenstein et al. 2007a, b), and two crystal structures of ADP-bound $MetN_2I_2$ in the inward-facing conformation without the substrate-binding protein MetQ bound (Johnson et al. 2012). The structure of the $ModB_2C_2$-A complex is similar to that of $MalFGK_2$ in the resting state, with the NBDs (ModC) in an open, nucleotide-free conformation and the TMDs (ModB) in an inward-facing conformation. ModC adopts a post-hydrolysis conformation and two molecules of inorganic phosphate are bound at the position of the β-phosphate groups of ATP in the ATP-bound structure of MalFGK-MBP (Oldham et al. 2007), suggesting that binding of a phosphate group at this position is probably the strongest compared to the position of the α- or γ-phosphate group.

Two pairs of crystal structures of the methionine transporter $MetN_2I_2$ from *E. coli* are available (Kadaba et al. 2008; Johnson et al. 2012), with the NBDs (MetN) spaced differently between the nucleotide-free and the ADP-bound structures. Similar to the structure of $MalFGK_2$ in the resting state, the MetN dimer is

held together by dimerization of the C-terminal domains. Each TMD contains five transmembrane segments, which correspond to TM4-8 of MalF and TM2-6 of MalG. The region of highest sequence and structure similarity is found at the region of the coupling helices and TM3 and TM4 located on either side of them. Similar to the maltose transporter, a network of salt bridges between the coupling helices of MetI and the helical subdomain of MetN relay the conformational changes between the TMD and NBD. The gate that closes the translocation cavity at the periplasmic side of $MetN_2I_2$ is structurally conserved and found in the $ModB_2C_2$ transporter.

Type II Importers

The Type II importers facilitate the uptake of metal chelates including vitamin B_{12}, heme, and oxanions (Klein and Lewinson 2011). For this group of ABC importers, seven crystal structures of complete transporters are available (Table 1). These structures correspond to five different states, which represent the major steps of the transport cycle. Five crystal structures are of the vitamin B_{12} transporter BtuCD from *E. coli* (Locher et al. 2002; Hvorup et al. 2007; Korkhov et al. 2012a, b, 2014), which is the most studied Type II importer. The two other crystal structures are of the molybdate/tungstate transporter $MolB_2C_2A$ from *Haemophilus influenzae* (Pinkett et al. 2007) and the heme transporter HmuUV from *Yersinia pestis* (Woo et al. 2012).

In 2002, the vitamin B_{12} transporter BtuCD from *E. coli* was crystallized in an outward-facing conformation, forming a cavity accessible from the periplasmic side (Locher et al. 2002). No substrate or nucleotides are bound and this outward-facing conformation probably represents the resting state of the transport cycle. The BtuC subunit consists of ten transmembrane helices, of which TM2-5 and TM7-10 are related by a pseudo-twofold rotation axis. Within the BtuC dimer, there is a twofold symmetry axis running down the translocation pathway. This translocation pathway is lined by residues from TM5, TM5a (small transmembrane helix following TM5), and TM10 of each BtuC, and the loops preceding TM3 and TM8. In this outward-facing conformation, the translocation cavity stretches out two-thirds into the predicted membrane and is closed by cytoplasmic gate I.

Given the millimolar ATP concentration in the cell, the resting state of the transporter will be short lived. The BtuDs will quickly bind ATP and the transporter will convert into an outward-facing, nucleotide-bound state as represented by the recently solved crystal structure of BtuCD in complex with two molecules of the non-hydrolyzable ATP analog AMP-PNP and two Mg^{2+} ions (Korkhov et al. 2014). Like in the resting state, the BtuC dimer is in an outward-facing conformation with a translocation cavity open to the periplasmic side but closed at the cytoplasmic side by a second cytoplasmic gate, known as cytoplasmic gate II. The BtuDs form a closed dimer with the AMP-PNP molecules and Mg^{2+} ions bound at the ATP hydrolysis site; in this state the two coupling helices of the BtuCs are about 9.5 Å closer to each other compared to the resting state. Apparently, the binding of

AMP-PNP promotes closure of the BtuD dimer, which is coupled to opening of cytoplasmic gate I and closure of cytoplasmic gate II in BtuC.

In the next step of the transport cycle, the substrate-binding protein BtuF binds vitamin B_{12} and subsequently docks onto the periplasmic side of the BtuC dimer. A study with BtuCD reconstituted in proteoliposomes has shown that ATP binding promotes docking of BtuF onto the BtuCD complex, rather than simulating BtuF release to scavenge vitamin B_{12} (Korkhov et al. 2014). Upon docking of BtuF onto the BtuCD complex, the N-terminal and C-terminal lobe of BtuF are spread apart while making interactions with periplasmic loops of BtuC. TM5a of BtuC sticks into the vitamin B_{12} binding site of BtuF, and this distortion forces vitamin B_{12} to move into the translocation cavity. Rearrangements within the BtuC dimer will then result in a substrate-bound, occluded state, which has been obtained in the presence of AMP-PNP (Korkhov et al. 2012b). In this state, the BtuD dimer closely resembles the previous state, but TM5 and TM5a of both BtuC subunits have now closed the translocation cavity from the periplasmic side, while cytoplasmic gate II is still closed. Although vitamin B_{12} is not present in this crystal structure, the cavity is wide enough to host the molecule with only minor steric hindrance. The interior of the cavity does not resemble the substrate-binding pocket of BtuF, rather it forms a low-affinity chamber.

After hydrolysis of ATP, the cytoplasmic gate II in the BtuD dimer will open to release inorganic phosphate and ADP. The substrate may then be squeezed out by a peristaltic-like movement. The state after substrate release is visualized by the crystal structure of the molybdate/tungstate transporter $MolB_2C_2$ from *Haemophilus influenzae* (Pinkett et al. 2007). The transporter was crystallized in a nucleotide-free, inward-facing conformation in the absence of the substrate-binding protein MolA. The arrangement of the transmembrane helices of MolB is similar to that of BtuC. In $MolB_2C_2$ only the TM5a of each subunit contributes to the formation of the periplasmic gate. EPR and selective crosslinking studies show that this gate offers a narrower opening upon nucleotide binding compared to the periplasmic gate in BtuCD, which is in agreement with the much smaller substrates molybdate or tungstate as compared to vitamin B_{12} (Rice et al. 2013).

To return to the outward-facing resting state, BtuF should dissociate and cytoplasmic gate I should close while the periplasmic gate needs to open up. A post-translation, intermediate state was crystallized in two different asymmetric conformations (Hvorup et al. 2007; Korkhov et al. 2012a). While the two non-identical lobes of BtuF interact with the periplasmic loops of the BtuC subunits, a slight asymmetry is introduced in the loops, resulting in an asymmetric arrangement of the transmembrane helices. Especially the orientation of TM3-5a is thought to control on which side of the membrane the translocation cavity is opened. The closure of the periplasmic gate and cytoplasmic gate I ensures that no continuous channel is formed, while switching from the inward-facing to the outward-facing conformation. Once the transporter reaches the outward-facing conformation by opening the periplasmic gate, BtuF will be released and the transporter is back in the resting state.

Type III Importers

Compared to the Type I and Type II importers, the structural information on the Type III importers/ECF transporters is limited. To date, crystal structures of four different S-components (Zhang et al. 2010; Erkens et al. 2011; Berntsson et al. 2012; Yu et al. 2014), two NBD dimers (Chai et al. 2013; Karpowich and Wang 2013), and three complete transporters are available (Xu et al. 2013; Wang et al. 2013; Zhang et al. 2014) (Table 1). The four substrate-bound S-components are RibU for riboflavin from *Staphylococcus aureus* (Zhang et al. 2010), ThiT for thiamin and BioY for biotin from *Lactococcus lactis* (Erkens et al. 2011; Berntsson et al. 2012), and NikM2 for Ni^{2+} for *Thermoanaerobacter tengcongensis* (Yu et al. 2014).

S-components. RibU, ThiT, and BioY associate with group II ECF transporters and despite a sequence identity of only 14–16 %, these S-components share a common structural fold of a six transmembrane helical bundle. The N-terminal parts consisting of TM1-3 are structurally the most conserved and were predicted to be involved in the interaction with the ECF module. TM1 contains a conserved AxxxA motif, which is important for complex formation and thiamin transport by ECF ThiT from *L. lactis* (Erkens et al. 2011) and biotin transport by the group I transporter BioMNY from *Rhodobacter capsulatus* (Finkenwirth et al. 2015). TM4-6 in the C-terminal parts of S-components are structurally more different and are the main contributors to the substrate-binding site. This combination of a structurally conserved part and a highly divergent part explains how different S-components can interact with one and the same ECF module and maintain a high specificity for chemically diverse substrates (dissociation constants in the sub-nanomolar to nanomolar range). The substrate-binding pocket is located on the predicted extracytoplasmic side of the S-component and closed by the L1 loop connecting TM1 and TM2, which lies over the pocket in a lid-like manner. EPR studies on thiamin-specific ThiT from *L. lactis* have shown that the main difference between thiamin-bound and substrate-free ThiT is the conformation of this L1 loop, covering the substrate-binding pocket in the liganded state, while exposing it to the environment in the unliganded state (Majsnerowska et al. 2013).

NikM2 is the S-component of the NikM2N2OQ transporter from *T. tengcongensis*, which is a metal transporter of the group I ECF transporters (Yu et al. 2014). Compared to the three vitamin-specific S-components, NikM2 has an additional N-terminal α-helix. The highly conserved extracellular N-terminus inserts into the center of the S-component and occupies a space that corresponds to the substrate-binding pocket in the vitamin-specific S-components. Within this space, Ni^{2+} is bound in a square-planar geometry by four nitrogen atoms. The nickel-binding residues are stabilized and oriented by a network of hydrogen bonds.

Full-length transporters. The structures of the complete Type III transporters all show the same conformation, in which the EcfAA' heterodimer adopts an open conformation and the substrate-free S-components lie in the membrane with the helical axis almost perpendicular to the plane of the membrane (Fig. 6). These

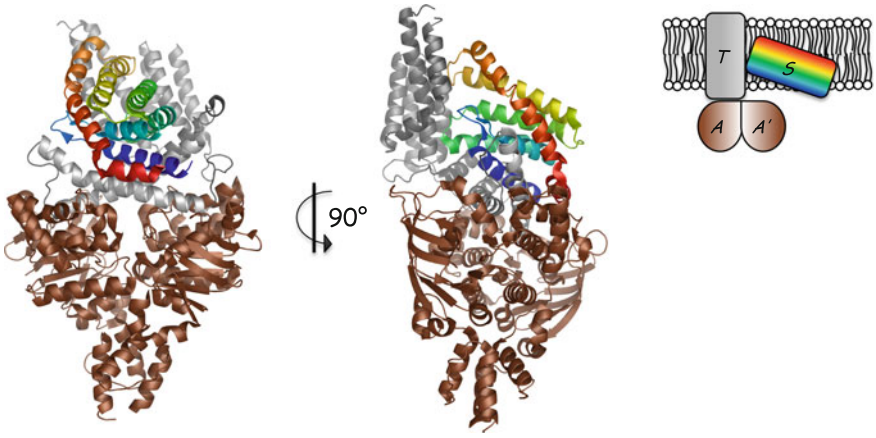

Fig. 6 Crystal structure of a Type III ABC importer. The crystal structure of ECF FolT is shown in the secondary-structure representation from the plane of the membrane from two sides, related by rotation of 90°. The two NBDs are colored in *brown*, EcfT is colored in *gray* and the S-component is colored from the N-terminus in *blue* to the C-terminus in *red*. In the *upper-right corner*, a schematic representation showing all subunits in the same color code is given to indicate the position of the membrane. The figure was generated with PyMoL, using structure PBD ID: 4HUQ

transporters have the same ECF module in complex with three different S-components: FolT for folate (Xu et al. 2013), PanT for pantothenate (Zhang et al. 2014), and HmpT; the latter is thought to bind pyridoxine (and should therefore be named PdxU) (Wang et al. 2013). The NBDs have the same structural fold as in Type I and Type II importers, including the RecA-like domain, the helical domain, and a C-terminal domain. All the conserved features (Walker A, Walker B, LSGGQ signature motif, D-, H-, and Q-loop) are present. A C-terminal extra domain provides the basis for dimerization (Chai et al. 2013; Karpowich and Wang 2013). Like the NBDs of the Type I and Type II importers, both dimers have two grooves at the interface of the RecA-like domain and the helical domain within one ATPase subunit, which can form the anchor points of eventual coupling helices. These acidic and highly conserved grooves are followed at the end of the Q-loop by a short 3_{10} helix, which seems to be conserved among the ECF transporters. This Q-helix has a conserved xPD/ExQφ (φ is a hydrophobic residue) motif, in which the conserved acidic residue and the conserved glutamine point to opposite sides of the helix. The latter points into the groove and is therefore thought to play a role in the interaction with transmembrane domains. The structures of the complete transporter also reveal a L-shaped EcfT consisting of eight α-helices, of which five are transmembrane helices (TM1-4 and TM8). Helix 5 lies at the cytoplasmic side of EcfT almost perpendicular to the transmembrane helices and helices 6 and 7 form two cytoplasmic coupling helices, which stick with their C-terminal ends into the grooves at the surface of EcfA' and EcfA, respectively. Together these coupling helices form a X-shaped bundle, which is stabilized by extensive hydrophobic interactions and hydrogen bonds between the conserved Glu174 in helix 6 and the

conserved Ser211 and Arg215 in helix 7. The C-terminal end of these helices is formed by a conserved XRX motif, in which the first X is usually an alanine and the second a glycine or serine (Neubauer et al. 2009). This signature motif participates in the interaction with the NBDs, and the interaction network is probably used to transfer conformational changes upon ATP binding and hydrolysis in the EcfAA' dimer to the transmembrane domains of the transporter.

In the transmembrane part of the transporter, the S-components bind in the cleft of the L-shaped EcfT, being separated from the EcfAA' dimer only by the coupling helices. Not TM1-3 which were predicted to interact with the ECF module, but TM1, TM2, and the C-terminal end of TM6 of all three S-components show a common surface, through which they interact with the coupling helices. The first coupling helix of EcfT mainly interacts with TM1 of the S-components via hydrophobic interactions and the AxxxA motif. The second coupling helix lies in a hydrophobic groove formed by TM1, TM2, and the C-terminal end of TM6 of the S-components. A similar groove is found in RibU, ThiT, and BioY. TM1, TM2, and the C-terminal end of TM6 contain several small hydrophobic residues that form an extensive hydrophobic interaction network with small hydrophobic residues in the coupling helix. This interaction network is important for the formation and stabilization of the whole transporter (Zhang et al. 2014). A second interaction site is formed by hydrophobic residues in the L3 and L5 loops of the S-components and hydrophobic residues in TM1, TM3, and TM4 in EcfT.

Mechanism of Transport

Type I Importers

The maltose transporter MalFGK$_2$E from *E. coli* is the best-studied Type I importer (Davidson et al. 2008; Oldham et al. 2007). In fact, a lot of what we know of full-length Type I ABC transporters comes from crystal structures of MalFGK$_2$-MBP, elucidated by the Davidson and Chen labs. Currently, structures of the maltose transporter in the inward-facing *apo*-state without the maltose-binding protein (MBP) (S_V in Fig. 7; Khare et al. 2009; Chen et al. 2013); in the outward-facing state with maltose, nucleotides, and MBP bound (S_{IV} in Fig. 7; Oldham et al. 2007; Oldham and Chen 2011b); and a pre-translocation state between the inward-facing and outward-facing state, with maltose and MBP bound and in the presence ($S_{III} \rightarrow S_{IV}$ in Fig. 7; Oldham and Chen 2011a) and absence of nucleotides ($S_{III} \rightarrow S_{IV}$ in Fig. 7; Oldham et al. 2013) are available. However, there is not yet a crystal structure of the nucleotide-bound inward-facing conformation (S_I–S_{III} in Fig. 7).

In growing cells, the levels of ATP (typically millimolar) are well above the K_D for binding of ATP to the NBDs and this primes the translocator for import (Fig. 7, $S_V \rightarrow S_I$). In S_I the translocator is in the nucleotide-bound inward-facing

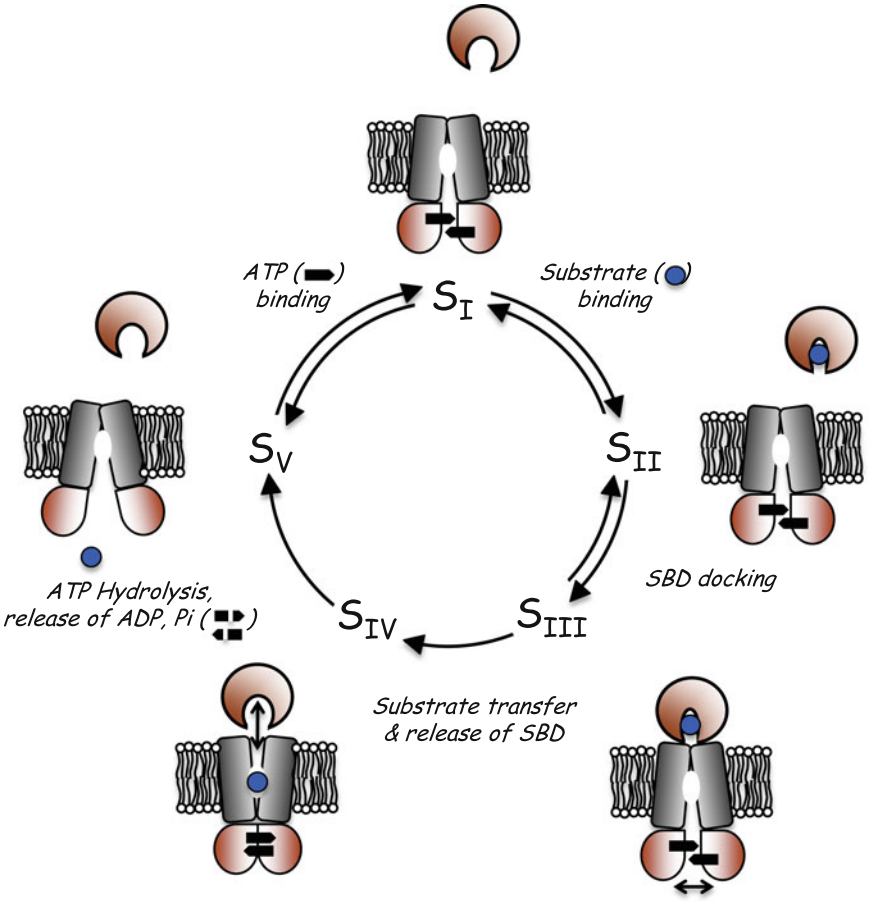

Fig. 7 Model of substrate translocation via a Type I ABC importer. After Gouridis et al. (2015)

conformation. Upon substrate capture via induced fit, the SBP changes conformation from open to closed (S_{II}) and, subsequently, docks onto the translocator (S_{III}). Through the binding of SBP in the CL state to the TMDs and Mg–ATP bound in the NBDs, the so-called pre-translocation state is formed (S_{III}), that is, the NBDs come closer together, forming a tipping for the access of the binding site in the TMDs. The binding energy of both ATP and SBP is used to transit the translocator from an inward to an outward-facing conformation ($S_{III} \rightarrow S_{IV}$), which allows the transfer of the substrate from the SBP to the TMD (S_{IV}). Subsequent hydrolysis of ATP and release of ADP and inorganic phosphate (Pi) complete the reaction cycle and release the substrate on the *trans* side of the membrane ($S_{IV} \rightarrow S_V$).

In another model of a Type I importer (Bao and Duong 2013), based on biochemical studies of the maltose transporter, the open state of the SBD interacts with the TMD in the outward-facing conformation, which then allows the binding of maltose. Upon subsequent hydrolysis of ATP, the transporter converts to the inward-facing conformation and releases the maltose into the cytoplasm. This model finds little support in the work on other Type I ABC importers, and the initiation of translocation through binding of SBP in the open state is controversial. In fact, the model of the Duong lab is based on studies in nanodiscs in which the coupling between maltose-MBP binding and ATP hydrolysis is relatively poor compared what others measure (Alvarez et al. 2010), and $MalFGK_2$-MBP may not have been in a fully native conformation.

An outstanding question is whether substrate recognition (selectivity) by ABC importers is counted for solely by the SBP or whether the TMD also contributes. For the maltose system there is data (Ferenci 1980; Ferenci et al. 1986; Treptow and Shuman 1985) suggesting that part of the selectivity originates from the TMD. For instance, mutants that function independent of the maltose-binding protein still transport no sugars other than maltodextrins (Treptow and Shuman 1985). In a recent structural study by the Chen lab (Oldham et al. 2013), it was shown that the transmembrane subunit MalF binds three glucosyl units from the non-reducing end of the sugar, suggesting that both MBP and the TMD contribute to the selectivity of the transporter. In accordance with these observations, the final step in translocation (Fig. 7, $S_{IV} \rightarrow S_V$) by GlnPQ is faster for asparagine than for glutamine (Gouridis et al. 2015). This implies that the two amino acids interact differently with the TMD and that additional selectivity to transport is provided beyond the step of substrate binding to the SBDs.

Another point of discussion is the stoichiometry of the transport reaction, which is technically challenging to determine. Many ABC transporters display poor coupling between ATP hydrolysis and translocation when purified and reconstituted in lipid vesicles, that is, significant amounts of ATP are hydrolyzed even in the absence of substrate. Another difficulty is that the substrate and ATP need to be present on opposite sides of the membrane, and the affinity of the TMD for the SBP is low (Prossnitz et al. 1989; Dean et al. 1992; Doeven et al. 2004). The Type I ABC importer OpuA transports glycine betaine and is gated by ionic strength. Like GlnPQ it has the SBD covalently linked (Fig. 3), which facilitates the membrane reconstitution and the ability to perform functional assays. Importantly, below threshold levels of ionic strength, there is hardly any ATP hydrolysis provided the lipid composition is "physiological" (>25 mol% of anionic lipids, 40–50 % non-bilayer lipids) (van der Heide et al. 2001; Biemans-Oldehinkel et al. 2006a). Under these conditions and upon activation of the transporter, the experimental ATP/glycine betaine ratio was 2.0 ± 0.5 (Patzlaff et al. 2003), suggesting a mechanistic stoichiometry of 2. At present, this is probably the best estimate of the ATP/substrate ratio for any ABC transporter.

A subset of ABC importers has additional domains fused to the NBDs, which serve to control the activity of the transporter. $MalFGK_2$-MBP from *E. coli* and OpuA from *Lactococcus lactis* are the best-studied systems in terms of regulation of

transport. The C-terminal domain of MalK of the maltose transporter is involved in carbon catabolite repression (Böhm et al. 2002), which determines the hierarchy of sugar utilization and is also known as an inducer exclusion mechanism. The C-terminal domain of MalK can interact with IIA^{glc}, a component of the bacterial phosphoenolpyruvate-dependent sugar phosphotransferase system (PTS). IIA^{glc} can be in the unphosphorylated and phosphorylated states, depending on the availability of PTS sugars (Nelson and Postma 1984; Dean et al. 1991). In the unphosphorylated form, i.e., when a PTS sugar such as glucose is present, IIA^{glc} binds to MalK and thereby prevents uptake of maltose, the inducer of the maltose operon. It has been recently shown that IIA^{glc} stabilizes the inward-facing conformation of the maltose transporter by wedging between the NBD of one MalK and the regulatory domain of the opposite MalK (Chen et al. 2013). Herewith, the closure of the NBDs and thus the formation of the outward-facing conformation are prevented, which are key steps for ATP hydrolysis and maltose translocation. The inhibition is relieved when glucose is exhausted and IIA^{glc} becomes phosphorylated.

The activity of OpuA increases with the osmolality of the medium, which is signaled to the protein as an increase in the cytoplasmic electrolyte concentration (gating by ionic strength). Two cystathionine-β-synthase (CBS) domains fused in tandem (CBS module) to the C-terminus of the NBD and an anionic membrane surface are central to the gating of the transporter by ionic strength (Biemans-Oldehinkel et al. 2006b; Karasawa et al. 2013). CBS2 is involved in electrolyte sensing, whereas the CBS1 domain merely serves as linker between the nucleotide-binding domain (NBD) and the CBS2 domain (Karasawa et al. 2011). In one model the interaction of the CBS module with an anionic membrane surface locks the transporter in an inactive conformation. Increasing the intracellular ionic strength beyond threshold levels screens the electrostatic interactions of oppositely charged surfaces and activates the transporter. Alternatively, the ionic gating of OpuA could involve two like-charged surfaces, such as the anionic membrane and anionic protein residues, in which case a high ionic strength would promote their interaction. The verdict is not yet out but it is evident that screened electrostatic forces and an anionic membrane surface are intrinsic to the gating mechanism of OpuA.

For a number of Type I ABC transporters, it has been observed that *trans*-accumulated substrate inhibits the translocation. In *Listeria monocytogenes* and *Lactobacillus plantarum*, the transport of glycine betaine and carnitine is inhibited by pre-accumulated (*trans*) substrate at 0.1 M or above (Verheul et al. 1997; Glaasker et al. 1998). Upon raising the medium osmolality, the corresponding ABC transporters are rapidly activated through a diminished *trans*-inhibition. Once cellular osmostatic conditions are restored, the transporters are switched off. This so-called *trans*-inhibition serves as a control mechanism to prevent the accumulation of the compatible solutes glycine betaine and carnitine to too high levels and thereby prevents the turgor pressure from becoming too high. Although the physiological effect is the same, *trans*-inhibition is mechanistically different from the ionic strength gating observed in OpuA. The ABC transporter OpuA is not inhibited by *trans*-substrate up to at least 400 mM (Patzlaff et al. 2003). For two

Type I ABC transporters the structural basis for *trans*-inhibition has been elucidated, that are the methionine transporter MetN2I2 from *E. coli* and the molybdate transporter ModB2C2 from *Methanosarcina acetivorans*. In both cases, the NBD subunits have a C-terminal regulatory domain albeit with distinct folds (Gerber et al. 2008; Johnson et al. 2012). The MetN2I2 system is inhibited when cytoplasmic levels of methionine reach threshold values (Kadner 1977), and the binding of methionine to the C-terminal domain stabilizes the transporter in the inward-facing conformation, similar to what IIA^{glc} does to the maltose transporter. The ModB2C2 system is inhibited by the binding of molybdate or tungstate to its C-terminal regulatory domain.

In summary: In recent years, we have obtained enormous insight into the energetics and mechanism of transport and selectivity for ligands, as well as the gating of a subset of Type I importers. The regulation of ABC transporters is typically affected through one or more additional domains, linked to the NBD, which allow the transporter to be fully switched off under certain nutrient or osmotic conditions, even if substrate and ATP are available.

Type II Importers

Type I and Type II importers differ in their architecture of the SBP and TMD, but also mechanistically these transporters appear to operate differently (Davidson et al. 2008; Rees et al. 2009; Lewinson et al. 2010; Joseph et al. 2011). The mechanism of transport by a Type II importer presented in Fig. 8 is based on crystal structures of each of the states (Korkhov et al. 2014). The vitamin B_{12} transporter BtuCDF from *E. coli* is the best-studied Type II importer (Locher et al. 2002), and most of the states are based on this transporter; state S_{III} is based on the structure of $MolB_2C_2$ from *Haemophilus influenzae* (Pinkett et al. 2007). The structural analysis suggests two cytoplasmic and one periplasmic gate(s), depicted as vertical (red) and horizontal (gray) bars, respectively (Fig. 8). S_I represents the nucleotide-bound, outward-facing conformation. Ligand-bound SBP docks onto the translocator and this results in an occluded state (S_{II}), following the diffusion of the ligand from the SBP to the TMD. Next, ATP is hydrolyzed and inorganic phosphate and ADP are released, which opens the cytoplasmic gate II and the substrate diffuses into the cytoplasm (S_{III}). The $S_{III} \rightarrow S_{IV}$ transition is only possible after the substrate has been released, as in the case of BtuCDF the cavity in the TMD has become too small to accommodate vitamin B_{12}. Korkhov et al. (2014) speculate that S_{IV} may prevent the back-reaction or non-specific solute transport through the translocation pathway. Next, the SBP dissociates from the translocator and the TMDs rearrange to form an outward-facing conformation (S_V). Given the high intracellular concentrations of ATP, S_V is rapidly converted into S_I; the ATP binding closes the cytoplasmic gate II and the system is reset for another translocation cycle.

The BtuCDF system has a very high apparent ATP/substrate stoichiometry, i.e., of the order of 50 (Borths et al. 2005), which may reflect a high rate of ATP

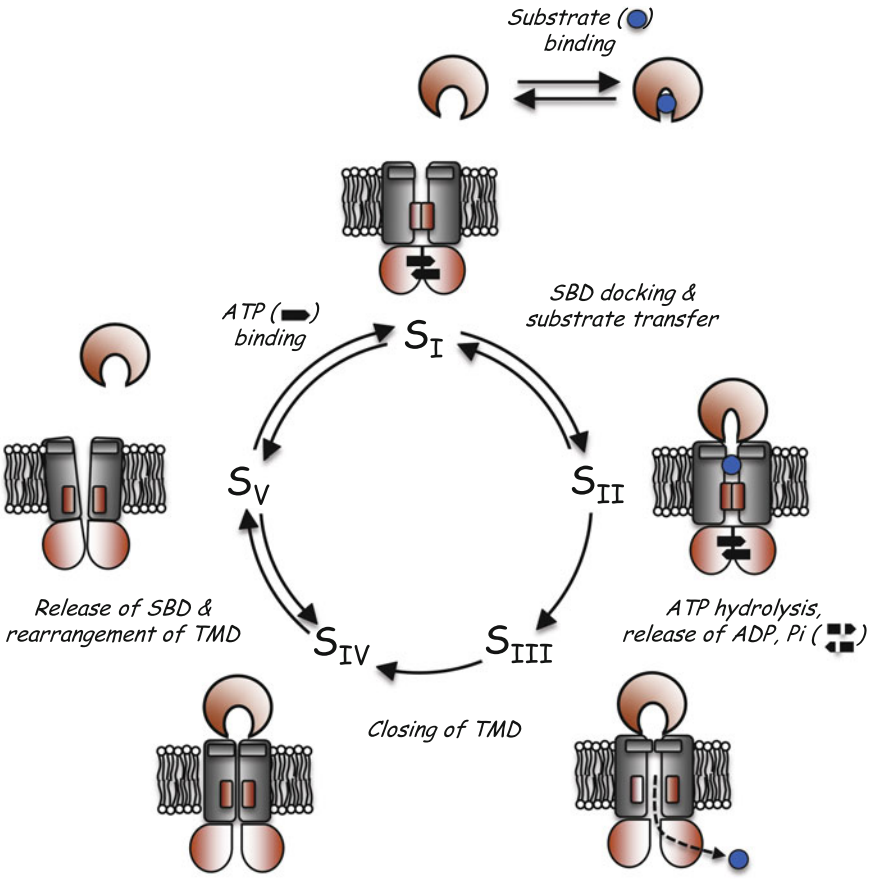

Fig. 8 Model of substrate translocation via Type II ABC importer. After Khorkhov et al. (2014)

hydrolysis of S_I or, as Korkhov et al. (2014) propose, S_{IV} to S_I-like transitions. This results in futile ATPase activity and a high apparent ATP/substrate stoichiometry; the mechanistic stoichiometry for full translocation is most likely 2. Contrary to the maltose transporter, there are no specific interactions between the substrate (vitamin B_{12}) and the TMD (BtuC subunits). The substrate pocket is very hydrophobic and forms a "Teflon-like" wall to prevent interactions with the hydrophilic substrate (Korkhov et al. 2012b). The NBDs of Type II importers discovered so far do not have extra domains and gating mechanisms (osmotic, catabolite, or product control) are not known.

In summary: Although Type I and Type II importers both employ extracytoplasmic SBPs or SBDs and operate by alternate access of the binding pockets in the TMDs, the mechanism of transport is very different. For instance, in the maltose transporter (Type I) the liganded SBP interacts with inward-facing TMD, whereas in the vitamin B_{12} transporter (Type II) the liganded SBP interacts with outward-facing

TMD. Accordingly, the subsequent steps are different for Type I and Type II importers.

Type III Importers

Apart from what has been revealed by the three crystal structures of the complete ECF FolT, ECF PantT, and ECF HmptT transporters from *L. brevis*, not much is known about the transport mechanism of the Type III importers. Unlike the Type I and Type II importers, the Type III importers contain a transmembrane domain that binds the substrate specifically without the help of a soluble SBP. At least 21 different S-component families are known, which are able to bind a wide range of small, chemically different substrates (Rodionov et al. 2006, 2009). Molecular dynamic simulation studies on the S-component ThiT for thiamin from *L. lactis* have shown that the six hydrophobic α-helices of the protein zig-zag through the lipid bilayer, with the connecting loops being located alternatively on the cytoplasmic and the extracellular side of it (Majsnerowska et al. 2013). In the four crystal structures of the substrate-bound S-components available, the substrate-binding site is located near the extracellular surface of the proteins (Zhang et al. 2010; Erkens et al. 2011; Berntsson et al. 2012; Yu et al. 2014). The site is formed by residues in the three C-terminal helices of the S-components together with residues in the L1 and L3 loops. These residues create specific, high-affinity binding sites with K_d values in the low nanomolar range (Erkens and Slotboom 2010; Zhang et al. 2010; Berntsson et al. 2012). The structure of the binding site of ThiT has been shown to be very robust, suggesting that a substantial input of energy, presumably in the form of ATP hydrolysis, is needed to accomplish conformational changes in the binding site to release its substrate (Swier et al. 2015). The N-terminal helices of the S-components are structurally more similar and provide interaction sites to interact with the EcfT domain. In the substrate-bound S-components, the substrate-binding site is closed by the L1 loop. However, in the structures of the complete transporters the L1 loop has moved away, opening the binding site to the cytoplasm (Wang et al. 2013; Xu et al. 2013; Zhang et al. 2014). This is in agreement with EPR studies performed on ThiT, which showed that the major difference between substrate-bound and substrate-free ThiT is a conformational change of the L1 loop (Majsnerowska et al. 2013).

In the structure of the complete transporters, the S-component adopts a highly unusual orientation, lying almost parallel in the membrane like it has toppled over from the orientation of the solitary S-components (S_I in Fig. 9) (Wang et al. 2013; Xu et al. 2013; Zhang et al. 2014). The S-component interacts with EcfT, but not with the NBDs, via two interaction sites with the interactions between TM1, TM2, and the C-terminal end of TM6 of the S-components and the coupling helices of EcfT forming the largest interaction interface. The two coupling helices create a X-shaped structure, of which the C-terminal ends stick into the grooves between the RecA-like domain and the helical domain at the surface of the EcfAA' dimer.

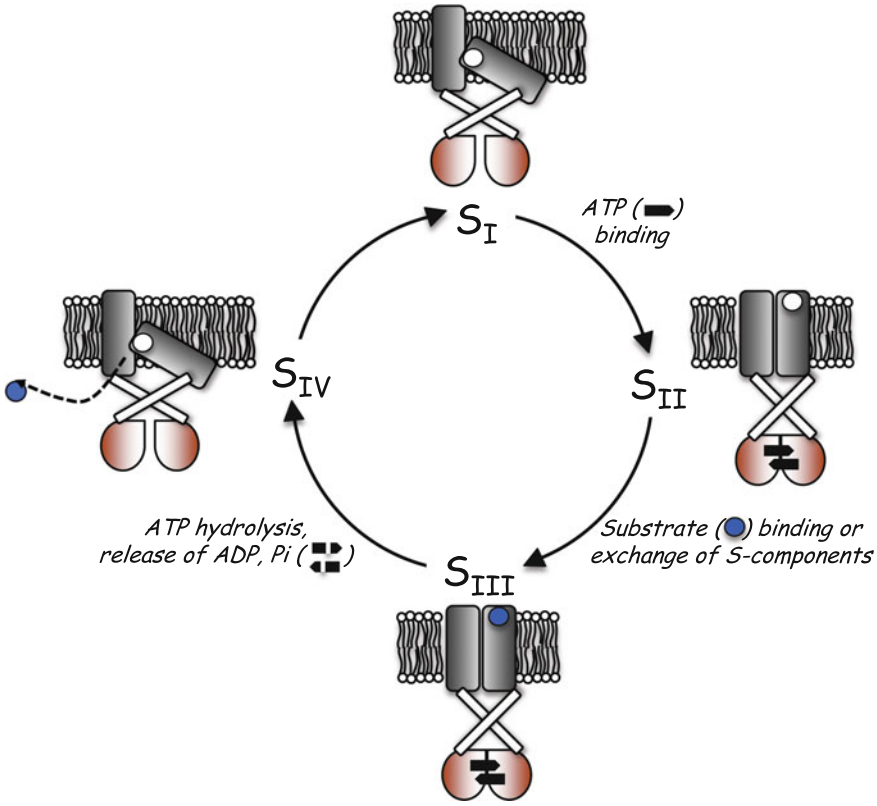

Fig. 9 Model of substrate translocation via a Type III ABC importer

Via an interaction network of electrostatic interactions and hydrogen bonds, these coupling helices are thought to transfer the conformational changes upon ATP binding and hydrolysis to the S-component. Like the NBDs in other ABC transporters, the EcfAA' dimer will undergo a tweezer-like closure upon ATP binding (S_{II} in Fig. 9) (Finkenwirth et al. 2015). This will probably push the C-terminal ends of the coupling helices together, creating a scissor-like conformation. The interactions between the S-component and EcfT are mainly hydrophobic (van der Waals), which allows the subunits to slide along each other. ATP binding might allow the S-component to rotate back to the up-right conformation in the membrane in order to capture its substrate on the extracytoplasmic side, while maintaining the interaction with EcfT (Finkenwirth et al. 2015). It is also possible that in this orientation, the interaction between the substrate-free S-component and EcfT is weakened and the two will dissociate, allowing another substrate-bound S-component to bind (S_{III} in Fig. 9) (Karpowich et al. 2015). Early research has shown that within the group II ECF transporters multiple S-components can compete for the same ECF module and that the affinity of the S-component for the

ECF module is dependent on the substrate concentration, with substrate-bound S-components binding stronger to EcfT than S-components in the absence of their substrate (Henderson et al. 1979). ATP hydrolysis and subsequent release of the hydrolysis products will then allow the coupling helices to move back to the open-scissor conformation and allow the S-component to topple over (S_{IV} in Fig. 9). The energy generated by ATP hydrolysis could be used to lower the binding affinity for the substrate, so it can be released into the cytoplasm. This mechanism would be new form of the moving-carrier mechanism, in which the S-component moves as a rigid body like in the elevator mechanism, but topples over to expose the substrate binding site to the cytoplasm, rather than making a translational movement as in the elevator mechanism.

A 1:1:1:1 stoichiometry was found in the crystal structures of the complete transporters and this stoichiometry has been confirmed by light scattering experiments performed on the group II ECF transporters from *L. lactis* (ter Beek et al. 2011). On the other hand, a 1:1:2:2 (A:A':T:S) stoichiometry was suggested for the group II riboflavin transporter from *Thermotoga maritima* (Karpowich and Wang 2013) and oligomeric EcfT and S-components were suggested for the group I biotin transporter from *Rhodobacter capsulatus* (Finkenwirth et al. 2010; Neubauer et al. 2011; Kirsch et al. 2012). The former result is difficult to reconcile with the crystal structures, but in the latter case it is possible that two or more complexes oligomerized in the membrane, and that the basic complex has 1:1:1:1 stoichiometry. Besides the debate on stoichiometry, rare solitary S-components have been found that seem to function independent of the ECF module, i.e., they are found in organisms that do not have the genes for the ECF module. An example is the biotin-specific S-component BioY, found in almost all Chlamydia strains, diverse proteobacterial and cyanobacterial species (Rodionov et al. 2009; Fisher et al. 2012; Finkerwirth et al. 2013). Furthermore, BioY and the cobalt-specific S-component CbiMN from *Rhodobacter capsulatus* may facilitate substrate entry into the cell in the absence of the ECF module (Hebbeln et al. 2007; Siche et al. 2010). Maybe these S-components topple over spontaneously in the membrane, a transition that would be energetically unfavourable but such rare events may suffice to allow the cell to take up small amounts of micronutrients. The S-components could also oligomerize and subsequently assist each other in the toppling in the membrane, or they could be assisted by unknown protein(s).

In conclusion: Type I and Type II ABC importers employ extramembranous substrate-binding proteins to capture their substrate and deliver the molecule to the translocator. Type III ABC importers use an integral membrane protein (S-component) for the initial binding of substrate; transport is thought to take place by reorientation of the S-component in the membrane. Whereas full structures of Type I and Type II ABC importers with/without SBPs are available, the translocation mechanism by Type III importers awaits further biochemical and structural analysis.

References

Alvarez FJ, Orelle C, Davidson AL (2010) Functional reconstitution of an ABC transporter in nanodiscs for use in electron paramagnetic resonance spectroscopy. J Am Chem Soc 132:9513–9515

Bao H, Duong F (2013) ATP alone triggers the outward facing conformation of the maltose ATP-binding cassette transporter. J Biol Chem 288:3439–3448

Berger EA, Heppel LA (1974) Different mechanisms of energy coupling for the shock-sensitive and shock-resistant amino acid permeases of *Escherichia coli*. J Biol Chem 249:7747–7755

Berntsson RP-A, Smits SH, Schmitt L, Slotboom DJ, Poolman B (2010) A structural classification of substrate-binding proteins. FEBS Lett 584:2606–2617

Berntsson RP-A, ter Beek J, Majsnerowska M, Duurkens RH, Puri P, Poolman B, Slotboom DJ (2012) Structural divergence of paralogous S components from ECF-type ABC transporters. Proc Natl Acad Sci USA 109:13990–13995

Biemans-Oldehinkel E, Doeven MK, Poolman B (2006a) ABC transporter architecture and regulatory roles of accessory domains. FEBS Lett 580:1023–1035

Biemans-Oldehinkel E, Mahmood NABN, Poolman B (2006b) A sensor for intracellular ionic strength. Proc Natl Acad Sci USA 103:10624–10629

Böhm A, Diez J, Diederichs K, Welte W, Boos W (2002) Structural model of MalK, the ABC subunit of the maltose transporter of *Escherichia coli*: implications for mal gene regulation, inducer exclusion, and subunit assembly. J Biol Chem 277:3708–3717

Borths EL, Poolman B, Hvorup RN, Locher KP, Rees DC (2005) In vitro functional characterization of BtuCD-F, the *Escherichia coli* ABC transporter for vitamin B-12 uptake. Biochemistry 44:16301–16309

Chai C, Yu Y, Zhuo W, Zhao H, Li X, Wang N, Chai J, Yang M (2013) Structural basis for a homodimeric ATPase subunit of an ECF transporter. Protein Cell 4:793–801

Chen S, Oldham ML, Davidson AL, Chen J (2013) Carbon catabolite repression of the maltose transporter revealed by X-ray crystallography. Nature 499:364–368

Clore GM (2014) Interplay between conformational selection and induced fit in multidomain protein-ligand binding probed by paramagnetic relaxation enhancement. Biophys Chem 186:3–12

Davidson AL, Dassa E, Orelle C, Chen J (2008) Structure, function, and evolution of bacterial ATP-binding cassette systems. Microbiol Mol Biol Rev 72:317–364

Dean DA, Reizer J, Nikaido H, Saier MH Jr (1991) Regulation of the maltose transport system of *Escherichia coli* by the glucose-specific enzyme III of the phosphoenolpyruvate-sugar phosphotransferase system. Characterization of inducer exclusion-resistant mutants and reconstitution of inducer exclusion in proteoliposomes. J Biol Chem 265:21005–21010

Dean DA, Hor LI, Shuman HA, Nikaido H (1992) Interaction between maltose-binding protein and then membrane-associated maltose transporter complex in *Escherichia coli*. Mol Microbiol 6:2033–2040

Doeven MK, Abele R, Tampe R, Poolman B (2004) The binding specificity of OppA determines the selectivity of the oligopeptide ATP-binding cassette transporter. J Biol Chem 279:32301–32307

Erkens GB, Slotboom DJ (2010) Biochemical characterization of ThiT from *Lactococcus lactis*: a thiamin transporter with picomolar substrate binding affinity. Biochemistry 49:3203–3212

Erkens GB, Berntsson RP-A, Fulyani F, Majsnerowska M, Vujičić-Žagar A, ter Beek J, Poolman B, Slotboom DJ (2011) The structural basis of modularity in ECF-type ABC transporters. Nature Struct Mol Biol 18:755–760

Ferenci T (1980) Methyl-α-maltoside and 5-thiomaltose: analogs transported by the *Escherichia coli* maltose transport system. J Bacteriol 144:7–11

Ferenci T, Muir M, Lee KS, Maris D (1986) Substrate specificity of the *Escherichia coli* maltodextrin transport system and its component proteins. Biochim Biophys Acta 860:44–50

Finkenwirth F, Neubauer O, Gunzenhäuser J, Schoknecht J, Scolari S, Stöckl M, Korte T, Herrmann A, Eitinger T (2010) Subunit composition of an energy-coupling-factor-type biotin transporter analysed in living cells. Biochem J 431:373–380

Finkenwirth F, Kirsch F, Eitinger T (2013) Solitary BioY proteins mediate biotin transport into recombinant *Escherichia coli*. J Bacteriol 195:4105–4111

Finkenwirth F, Sippach M, Landmesser H, Kirsch F, Ogienko A, Grunzel M, Kiesler C, Steinhoff H-J, Schneider E, Eitinger T (2015) ATP-dependent conformational changes trigger substrate capture and release by an ECF-type biotin transporter. J Biol Chem (in press)

Fisher DJ, Fernández RE, Adams NE, Maurelli AT (2012) Uptake of biotin by Chlamydia Spp. Through the use of a bacterial transporter (BioY) and a host-cell transporter (SMVT). PLoS ONE 7:e46052

Fukami-Kobayashi K, Tateno Y, Nishikawa K (1999) Domain dislocation: a change of core structure in periplasmic binding proteins in their evolutionary history. J Mol Biol 286:279–290

Fulyani F, Schuurman-Wolters GK, Vujičić-Žagar A, Guskov A, Slotboom DJ, Poolman B (2013) Functional diversity of tandem substrate-binding domains in ABC transporters from pathogenic bacteria. Structure 21:1879–1888

Gerber S, Comellas-Bigler M, Goetz BA, Locher KP (2008) Structural basis of trans-inhibition in a molybdate/tungstate ABC transporter. Science 321:246–250

Glaasker E, Heuberger EHML, Konings WN, Poolman B (1998) Mechanism of osmotic activation of the quaternary ammonium compound transporter (QacT) of *Lactobacillus plantarum*. J Bacteriol 180:5540–5546

Gouridis G, Schuurman-Wolters GK, Ploetz E, Husada F, Vietrov R, de Boer M, Cordes T, Poolman B (2015) Conformational dynamics in substrate-binding domains influences transport in the ABC importer GlnPQ. Nature Struct Mol Biol 22:57–64

Hebbeln P, Rodionov DA, Alfandega A, Eitinger T (2007) Biotin uptake in prokaryotes by solute transporters with an optional ATP-binding cassette-containing module. Proc Natl Acad Sci USA 104:2909–2914

Henderson GB, Zevely EM, Huennekens FM (1979) Mechanism of folate transport in *Lactobacillus casei*: evidence for a component shared with the thiamine and biotin transport systems. J Bacteriol 137:1308–1314

Hollenstein K, Dawson RJ, Locher KP (2007a) Structure and mechanism of ABC transporter proteins. Curr Opin Struct Biol 17:412–418

Hollenstein K, Frei DC, Locher KP (2007b) Structure of an ABC transporter in complex with its binding protein. Nature 446:213–216

Hvorup RN, Goetz BA, Niederer M, Hollenstein K, Perozo E, Locher KP (2007) Asymmetry in the structure of the ABC transporter-binding protein complex BtuCD-BtuF. Science 317:1387–1390

Johnson E, Nguyen PT, Yeates TO, Rees DC (2012) Inward facing conformations of the MetNI methionine transporter: implications for the mechanism of transinhibition. Protein Sci 21:84–96

Joseph B, Jeschke G, Goetz BA, Locher KP, Bourdignon E (2011) Transmembrane gate movements in the type II ATP-binding cassette (ABC) importer BtuCD-F during nucleotide cycle. J Biol Chem 286:41008–41017

Kadaba NS, Kaiser JT, Johnson E, Lee A, Rees DC (2008) The high-affinity *E. coli* methionine ABC transporter: structure and allosteric regulation. Science 321:250–253

Kadner RJ (1977) Transport and utilization of D-methionine and other methionine sources in Escherichia coli. J Bacteriol 129:207–216

Karasawa A, Erkens GB, Berntsson RP-A, Otten R, Schuurman-Wolters GK, Mulder FA, Poolman B (2011) Cystathionine β-synthase (CBS) domains 1 and 2 fulfill different roles in ionic strength sensing of the ATP-binding cassette (ABC) transporter OpuA. J Biol Chem 286:37280–37291

Karasawa A, Swier LJYM, Stuart MC, Brouwers J, Helms B, Poolman B (2013) Physicochemical factors controlling the activity and energy coupling of an ionic strength-gated ABC transporter. J Biol Chem 288:29862–29871

Karpowich NK, Wang D-N (2013) Assembly and mechanism of a group II ECF transporter. Proc Natl Acad Sci USA 110:2534–2539

Karpowich NK, Song JM, Cocco N, Wang D-N (2015) ATP binding drives substrate capture in an ECF transporter by a release-and-catch mechanism. Nat Struct Mol Biol 22:565–571

Khare D, Oldham ML, Orelle C, Davidson AL, Chen J (2009) Alternating access in maltose transporter mediated by rigid-body rotations. Mol Cell 33:528–536

Kim E, Lee S, Jeon A, Choi JM, Lee HS, Hohng S, Kim HS (2013) A single-molecule dissection of ligand binding to a protein with intrinsic dynamics. Nature Chem. Biol. 9:313–318

Kirsch F, Freilingsdorf S, Pohlmann A, Ziomkowska J, Hermann A, Eitinger T (2012) Essential amino acid residues of BioY reveal that dimers are the functional S unit of the *Rhodobacter capsulatus* biotin transporter. J Bacteriol 194:4504–4512

Klein JS, Lewinson O (2011) Bacterial ATP-driven transporters of transition metals: physiological roles, mechanisms of action, and roles in bacterial virulence. Metallomics 3:1098–1108

Korkhov VM, Mireku SA, Hvorup RN, Locher KP (2012a) Asymmetric states of vitamin B12 transporter BtuCD are not discriminated by its cognate substrate binding protein BtuF. FEBS Lett 586:972–976

Korkhov VM, Mireku SA, Locher KP (2012b) Structure of AMP-PNP-bound vitamin B12 transporter BtuCD-F. Nature 490:367–372

Korkhov VM, Mireku SA, Veprintsev DB, Locher KP (2014) Structure of AMP-PNP-bound BtuCD and mechanism of ATP-powered vitamin B12 transport by BtuCD-F. Nature Struct Mol Biol 21:1097–1099

Lewinson O, Lee AT, Locher KP, Rees DC (2010) A distinct mechanism for the ABC transporter BtuCD-BtuF revealed by the dynamics of complex formation. Nature Struct Mol Biol 17:332–338

Locher KP, Lee AT, Rees DC (2002) The *E. coli* BtuCD structure: a framework for ABC transporter architecture and mechanism. Science 296:1091–1098

Majsnerowska M, Hänelt I, Wunnicke D, Schäfer LV, Steinhoff HJ, Slotboom DJ (2013) Substrate-induced conformational changes in the S-component ThiT from an energy coupling factor transporter. Structure 21:861–867

Manson M, Boos W, Bassford P, Rasmussen B (1985) Dependence of maltose transport and chemotaxis on the amount of maltose-binding protein. J Biol Chem 260:9727–9733

Nelson SO, Postma PW (1984) Interactions *in vivo* between III^{Glc} of the phosphoenolpyruvate:-sugar phosphotransferase system and the glycerol and maltose uptake systems of *Salmonella typhimurium*. Eur J Biochem 139:29–34

Neubauer O, Alfandega A, Schoknecht J, Sternberg U, Pohlmann A, Eitinger T (2009) Two essential arginine residues in the T components of energy-coupling factor transporters. J Bacteriol 191:6482–6488

Neubauer O, Reiffler C, Behrendt L, Eitinger T (2011) Interactions among the A and T units of an ECF-type biotin transporter analyzed by site-specific crosslinking. PLoS ONE 6:e29087

Oldham ML, Chen J (2011a) Crystal structure of the maltose transporter in a pretranslocation intermediate state. Science 332:1202–1205

Oldham ML, Chen J (2011b) Snapshots of the maltose transporter during ATP hydrolysis. Proc Natl Acad Sci USA 108:15152–15156

Oldham ML, Khare D, Quicho FA, Davidson AL, Chen J (2007) Crystal structure of a catalytic intermediate of the maltose transporter. Nature 450:515–521

Oldham ML, Chen S, Chen J (2013) Structural basis for substrate specificity in the Escherichia coli maltose transport system. Proc Natl Acad Sci USA 110:18132–18137

Patzlaff J, van der Heide T, Poolman B (2003) The ATP/substrate stoichiometry of the ABC transporter OpuA. J Biol Chem 278:29546–29551

Pinkett HW, Lee AT, Lum P, Locher KP, Rees DC (2007) An inward-facing conformation of a putative metal-chelate-type ABC transporter. Science 315:373–377

Prossnitz E, Gee A, Ames GFL (1989) Reconstitution of the histidine periplasmic transport-system in membrane-vesicles—energy coupling and interaction between the binding-protein and the membrane complex. J Biol Chem 264:5006–5014

Quiocho FA, Ledvina P (1996) Atomic structure and specificity of bacterial periplasmic receptors for active transport and chemotaxis: variation of common themes. Mol Microbiol 20:17–25

Quiocho FA, Phillips GN, Spurlino JC, Rodseth LE (1974) Crystallographic data of an L-arabinose-binding protein from *Escherichia coli*. J Mol Biol 86:491–493

Rees DC, Johnson E, Lewinson O (2009) ABC transporters: the power to change. Nature Rev Mol Cell Biol 10:218–227

Rice AJ, Alvarez FJD, Schultz KM, Klug CS, Davidson AL, Pinkett HW (2013) EPR spectroscopy of MolB2C2-A reveals mechanism of transport for a bacterial type II molybdate transporter. J Biol Chem 288:21228–21235

Rodionov DA, Hebbeln P, Gelfand MS, Eitinger T (2006) Comparative and functional genomics analysis of prokaryotic nickel and cobalt uptake transporters: evidence for a novel group of ATP-binding cassette transporters. J Bacteriol 188:317–327

Rodionov DA, Hebbeln P, Eudes A, ter Beek J, Rodionova IA, Erkens GB, Slotboom DJ, Gelfand MS, Osterman AL, Hanson AD, Eitinger T (2009) A novel class of modular transporters for vitamins in prokaryotes. J Bacteriol 191:42–51

Schuurman-Wolters GK, Poolman B (2005) Substrate specificity and ionic regulation of GlnPQ from *Lactococcus lactis*: an ATP-binding cassette transporter with four extracytoplasmic substrate-binding domains. J Biol Chem 280:23785–23790

Seo M-H, Park J, Kim E, Hohng S, Kim H-S (2014) Protein conformational dynamics dictate the binding affinity for a ligand. Nat Commun 5:3724

Siche S, Neubauer O, Hebbeln P, Eitinger T (2010) A bipartite S unit of an ECF-type cobalt transporter. Res Microbiol 161:824–829

Slotboom DJ (2014) Structural and mechanistic insights into prokaryotic energy-coupling factor transporters. Nature Rev Microbiol 12:79–87

Swier LJYM, Monjas L, Guskov A, Voogd de AR, Erkens GB, Slotboom DJ, Hirsch AKH (2015) Structure-based design of potent small-molecule binders to the S-component of the ECF transporter for thiamine. *ChemBioChem* published online ahead of print

ter Beek J, Duurkens RH, Erkens GB, Slotboom DJ (2011) Quaternary structure and functional unit of energy couplin factor (ECF)-type transporters. J Biol Chem 286:5471–5475

ter Beek J, Guskov A, Slotboom DJ (2014) Structural diversity of ABC transporters. J Gen Physiol 143:419–435

Treptow NA, Shuman HA (1985) Genetic-evidence for substrate and periplasmic-binding-protein recognition by the MalF and MalG proteins, cytoplasmic membrane-components of the *Escherichia-coli* maltose transport-system. J Bacteriol 163:654–660

van der Heide T, Poolman B (2002) ABC transporters: one, two or four extracytoplasmic substrate-binding domains? EMBO Rep 3:938–943

van der Heide T, Stuart MCA, Poolman B (2001) On the osmotic signal and osmosensing mechanism of an ABC transport system for glycine betaine. EMBO J 20:7022–7032

Verheul A, Glaasker E, Poolman B, Abee T (1997) Betaine and L-carnitine transport in response to osmotic signals in *Listeria monocytogenes* Scott A in response to osmotic signals. J Bacteriol 179:6979–6985

Vogt AD, Di Cera E (2013) Conformational selection is a dominant mechanism of ligand binding. Biochemistry 52:5723–5729

Wang T, Fu G, Pan X, Wu J, Gong X, Wang J, Shi Y (2013) Structure of a bacterial energy-coupling factor transporter. Nature 497:272–276

Woo J-S, Zeltina A, Goetz BA, Locher KP (2012) X-ray structure of the Yersinia pestis heme transporter HmuUV. Nature Struct Mol Biol 19:1310–1315

Xu K, Zhang M, Zhao Q, Yu F, Guo H, Wang C, He F, Ding J, Zhang P (2013) Crystal structure of a folate energy-coupling factor transporter from *Lactobacillus brevis*. Nature 497:268–271

Yu Y, Zhou M, Kirsch F, Xu C, Zhang L, Wang Y, Jiang Z, Wang N, Li J, Eitinger T, Yang M (2014) Planar substrate-binding site dictates the specificity of ECF-type nickel/cobalt transporters. Cell Res 24:267–277

Yu J, Ge J, Heuveling J, Schneider E, Yang M (2015) Structural basis for substrate specificity of an amino acid ABC transporter. Proc Natl Acad Sci USA 112:5243–5248

Zhang P, Wang J, Shi Y (2010) Structure and mechanism of the S-component of a bacterial ECF transporter. Nature 468:717–720

Zhang M, Bao Z, Zhao Q, Guo H, Xu K, Wang C, Zhang P (2014) Structure of a pantothenate transporter and implications for ECF module sharing and energy coupling of group II ECF transporters. Proc Natl Acad Sci USA 111:18560–18565